Hydrogen functionalization of graphene using RF plasma for photodetection

Ethan John Lim, Fu Wenbo, Qi Tianshi

1-15, 19HCI05

Abstract

The growth in fibre optic communication speeds, propelled by demand caused by ever-increasing data volumes, are limited by detector frequency response. Graphene-silicon Schottky diodes are a promising alternative to traditional photodetectors, with higher detection frequencies and higher light-to-dark current ratios. This study seeks to determine the optimal conditions − of proximity, duration, and power − for hydrogen functionalisation of graphene using chemical vapour deposition, which will be used to increase the barrier potential of the graphene-silicon diode, its main drawback compared to other photodiodes. Graphene was synthesised using chemical vapour deposition, and used to create a graphene-silicon Schottky diode. After hydrogen functionalisation, photocurrent measurements were done on graphene-silicon photodiodes while a light source shone pulses of light onto it, and the magnitude and spontaneity of the optoelectronic response were measured. Results showed that the intensity of optoelectronic response in graphene-silicon diodes is inversely related to its physical proximity to the plasma source during hydrogenation, and directly related to the power of the plasma, up to a point, after which it will deteriorate.

1 Introduction

The interface between graphene and silicon has been shown to form a Schottky barrier, which exhibits rectifying properties − only allowing current to flow in one direction, enabling its use as an electrical diode (Chen *et al*, 2011). Furthermore, graphene's optical transparency, along with its strong optoelectronic response, allows the generation of photocurrent by the graphene-silicon diode when absorbing light, making it suitable for use as a high-sensitive photodetector (Wang *et al*, 2013) with higher responsiveness and improved light-to-dark current ratio (An, Behnam, & Ural, 2013).

This brings great promise in the field of electronic communication, as graphene-based photodetectors have been shown to demonstrate multi-gigahertz operation over all fibre-optic telecommunication bands, exceeding existing commonly used germanium photodetectors (Pospischil *et al*, 2013). Deep sea fibre optic internet cables are carrying increasing amounts of data, requiring newer, faster networks to ensure speedy communication, thus graphene photodetectors have the potential to greatly improve fibre optics communications speeds, which currently faces low photodetection frequencies as one of the main drawbacks limiting its growth (Agrawal, 2012).

The main challenge of this application is that the barrier potential for graphene-silicon interface is lower than traditional metal-silicon junctions due to the low work function of graphene (Yan *et al*, 2012). Hydrogen plasma will be used to introduce defects onto the material surface, which will increase the barrier potential (Dey *et al*, 2016). Existing research has shown that nitrogen-doped graphene, grown through plasma-enhanced chemical vapour deposition using polydimethylsiloxane as the carbon source, can allow it to be used as the p-type layer in a diode (Wan *et al*, 2013).

2 Objectives and hypothesis

This study intends to:

- synthesise graphene using chemical vapour deposition (CVD) and create a graphene-silicon Schottky diode by transferring it onto a p-type silicon substrate; and
- investigate the optimal conditions (proximity to, power of, and duration of exposure to plasma) for hydrogen functionalisation that allows for the highest photodetection efficiency, as measured by strength and response time of photoelectric response.

This study hypothesises that:

- the graphene-silicon bilayer will display a strong photoelectric response when exposed to light, and will have higher detection frequency than traditional germanium-based photodetectors (greater than 25 GHz); and
- the photodetection efficiency of the graphene-silicon Schottky diode will be directly related to the power of the plasma and inversely related to the physical proximity and duration of exposure to the plasa source.

3 Experimental design and methodology

3.1 Synthesis of graphene-silicon diode

Few-layer graphene was synthesised using chemical vapor deposition (CVD), using methane gas as the carbon source. A 1 cm by 10 cm strip of copper was cleaned by sonication in acetone, IPA, then deionised water at 30°C for 10 minutes each. The copper strip was then placed on top of a graphene block, then into a Ø25 mm quartz tube, after which the internal pressure was reduced to 3.0 Pa (±4.0 Pa). Hydrogen gas was pumped into the tube at a rate of 2 cm^3 min^{-1}, while a heater was turned to 81.5W, 225W, then 386W at 30 minute intervals. When the temperature inside the tube reached 1100°C (± 50°C), methane gas was introduced at a rate of 10 cm^3 min^{-1}. After 1 hour, methane gas flow was stopped and the heater was turned off, allowing the tube to cool. When the temperature inside the tube reached room temperature, hydrogen gas flow was stopped and the pressure returned to ambient pressure. The graphene-coated copper strip was removed and stored in a humidity- and temperature-controlled cabinet. The CVD setup is shown in *Fig 1* in Appendix.

To create a graphene-silicon diode, the graphene layer was to be removed from the copper strip, then transferred onto a p-type silicon substrate. The graphene-coated copper strip was cut into 1 cm squares, then PMMA was spin-coated onto the graphene side. The copper squares were then placed onto the surface of concentrated iron(III) chloride solution, copper side down. When the copper was fully dissolved, the graphene/PMMA squares were lifted off the surface using glass slides, and placed onto the surface of deionised water to remove excess iron(III) chloride. 1 cm by 2 cm rectangles of p-type silicon were cut, then cleaned by sonication in acetone, IPA, then deionised water at 30°C for 10 minutes each. The graphene/PMMA squares were then lifted out of the water atop the cut and cleaned silicon pieces, then placed in an incubator at 80°C for 10 minutes to remove excess moisture. The silicon pieces were then placed in acetone to allow the PMMA to dissolve, leaving a graphene-silicon bilayer. The transfer process is shown in *Fig 2* in Appendix.

Raman spectroscopy and current-voltage (I-V) measurements were done on the graphene-silicon bilayer to ensure that few-layer graphene had been synthesised, and had formed a Schottky diode with the p-type silicon substrate.

3.2 Hydrogen functionalisation

Hydrogen functionalisation was explored as a potential method of increasing the barrier potential of the graphene-silicon diode. It involves doping the surface of graphene with hydrogen atoms using radio-frequency hydrogen plasma. The graphene-silicon diode was placed in a ceramic holder, then into a Ø25 mm quartz tube, after which the internal pressure was reduced to 100.0 Pa (±100.0 Pa). Hydrogen gas was pumped into the tube at a rate of 50 cm^3 min^{-1}, and current was then passed between two electrodes wrapped around the outside of the tube. The proximity of the diode to the electrodes, and the power and duration of the plasma were modified for each experiment. Once the required time had elapsed, the plasma and hydrogen gas flow were stopped, and pressure was returned to ambient pressure, after which the hydrogenated graphene-silicon diode was removed from the quartz tube. The hydrogenation setup is shown in *Fig 3* in Appendix.

The following variables were used during hydrogen functionalisation:

Independent variables	● Physical proximity from plasma electrodes ● Power of plasma ● Duration of exposure to plasma
Dependent variables	● Strength of photoelectric response ● Response time
Controlled variables	● Growth condition of graphene samples ● Silicon substrate

3.3 Current-voltage measurements

To determine the optoelectronic response the Schottky diode, I-V measurements were taken using an I-V machine. The cathode and anode of the I-V machine were placed onto the graphene and exposed silicon of the diode respectively. The environment around the diode was then darkened to reduce interference from other light sources on the results. A voltage bias test was then done on the diode, while an LED light above the diode was turned on and off at 10 second intervals. A graph of current against time was plotted based on experimental data, using which the difference in current in light and dark could be determined.

4 Results and discussion

4.1 Characterisation

4.1.1 Raman spectroscopy

Characterisation of graphene was done using Raman spectroscopy, where the graph obtained from the sample was compared with literature graphs for ideal graphene. Results are shown in *Fig 4a* and *Fig 4b*. *Fig 4b* clearly shows significant peaks from the D band, G band, and 2D band, as seen in the literature graph in *Fig 4a,* confirming the successful synthesis of few-layer graphene.

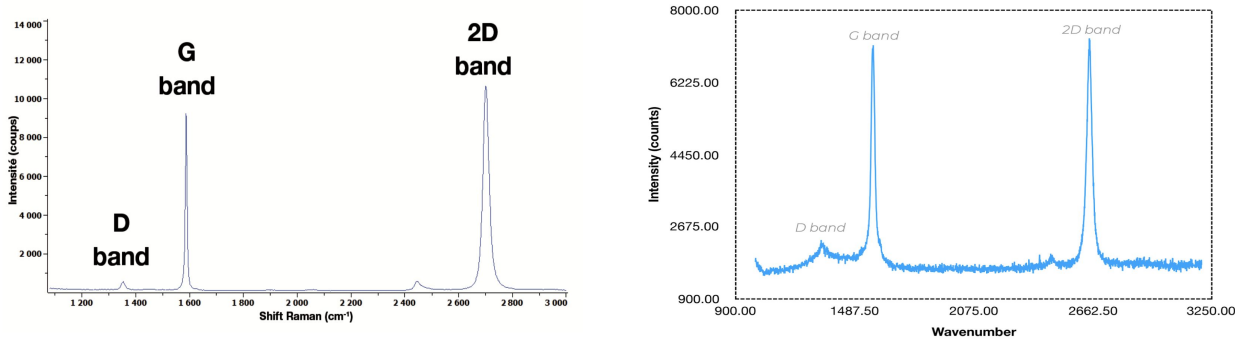

Fig 4a. (left) Raman graph for ideal graphene, obtained from literature

Fig 4b. (right) Raman graph obtained from synthesised graphene

4.1.2 IV characterisation

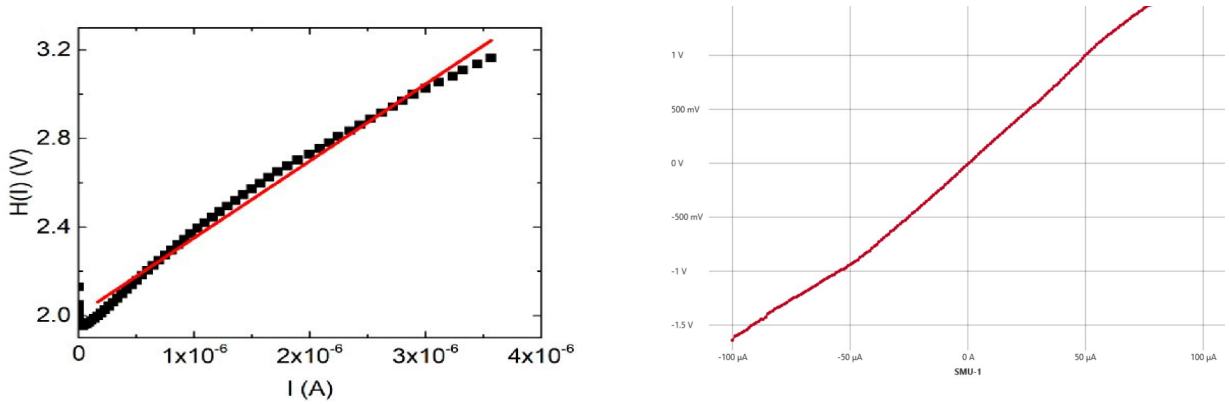

Fig 4c. (left) Literature I-V graph for ideal graphene. Fig 4d. (right) I-V graph obtained from synthesised graphene

I-V measurements were conducted on the synthesised graphene sample using an I-V machine, and compared with existing literature. *Fig 4d* shows that the synthesised graphene has a similar I-V graph to ideal graphene, showing that the synthesised graphene has similar electrical properties to graphene, suggesting the successful synthesis of few-layer graphene.

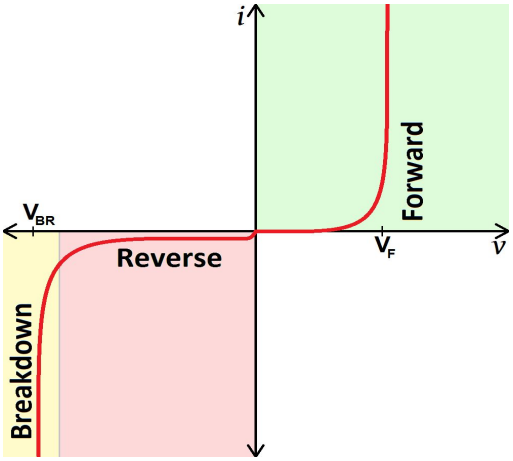

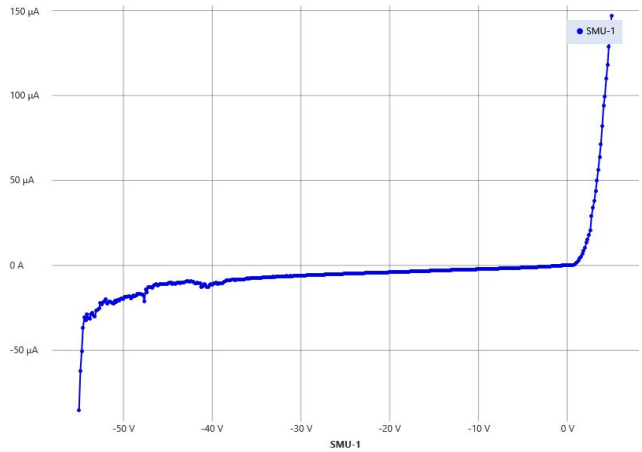

Fig 5a. (left) Literature I-V graph for ideal graphene-silicon diode

Fig 5b. (right) I-V graph obtained from synthesised graphene-silicon diode

To confirm that the graphene-silicon bilayer had successfully formed a Schottky diode, I-V measurements were conducted to determine its electrical properties, whose results are shown in *Fig 5a and Fig 5b*. The similar shapes of graphs from *Fig 5a* and *Fig 5b* show that the synthesised graphene demonstrates the expected electrical properties of an electrical diode, as seen from the sudden increase in current once the forward voltage was reached, and the backwards flow of current at the breakdown voltage. The synthesised diode has the added benefit of having a relatively low forward and breakdown voltage, hence allowing lower forward voltages to pass through and being more resistant to electrical flow in the reverse direction.

4.1.3 Ultraviolet photoelectron spectroscopy

The graphene samples on P-type silicon were examined under Ultraviolet photoelectron spectroscopy to characterise the graphene sample synthesised.

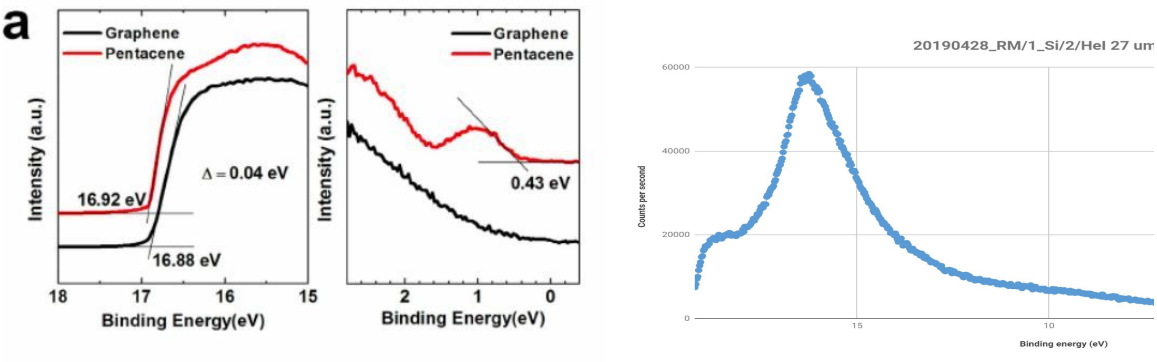

Fig 6a. (left) Literature UV photoelectron spectroscopy graph obtained from literature.

Fig 6b. (right) UV photoelectron spectroscopy graph obtained from sample.

Comparing the UV photoelectron spectroscopy graph from literature with that for the sample, it is possible to see that the sample has the same binding energy at approximately 16 eV, hence showing that graphene has been successfully synthesised.

4.2 Hydrogen functionalisation

For each experiment, to obtain the mean difference between the current measured in high and low light intensity environments, the average of all light-off data values was subtracted from the average of all light-on data values.

proximity / cm	**duration / min**	**power / W**	**mean difference / A**
-	-	-	8.46×10^{-8} (control)

Physical proximity test

proximity / cm	**duration / min**	**power / W**	**mean difference / A**
1	10	100	5.72×10^{-7} (highest)
5	10	100	6.85×10^{-8}
10	10	100	3.37×10^{-8} (lowest)

Exposure duration test

proximity / cm	**duration / min**	**power / W**	**mean difference / A**

5	10	100	6.85×10^{-8}
5	15	100	5.77×10^{-8} (lowest)
5	20	100	1.07×10^{-7} (highest)

Plasma power test

proximity / cm	**duration / min**	**power / W**	**mean difference / A**
5	10	50	7.46×10^{-9}
5	10	80	5.12×10^{-9}
5	10	90	1.95×10^{-7} (highest)
5	10	100	6.85×10^{-8}
5	10	110	1.95×10^{-7}
5	10	120	4.93×10^{-9}
5	10	150	7.36×10^{-10} (lowest)

Table 1. Experimental results

Based on the experimental results, it is possible to conclude that the mean difference between light and dark current generated by the graphene-silicon diode is directly related to its physical proximity to the plasma source during hydrogen functionalisation. This is likely because closer proximity to the plasma source will result in higher exposure of the diode to hydrogen plasma, therefore encouraging doping of hydrogen atoms.

Reliable conclusions were unable to be made to establish the relationship between duration of exposure and strength of optoelectronic response due to a lack of conclusive data, and further experimentation is required to allow conclusions to be drawn.

It is also possible to conclude that, up to a point, mean difference between current generation in light and dark conditions is inversely related to the power of the plasma used, but after which the optoelectronic response deteriorated again. This is likely because the higher power of plasma gives more energy for the formation of covalent bonds between carbon and hydrogen atoms, but too high-powered plasma will damage the graphene.

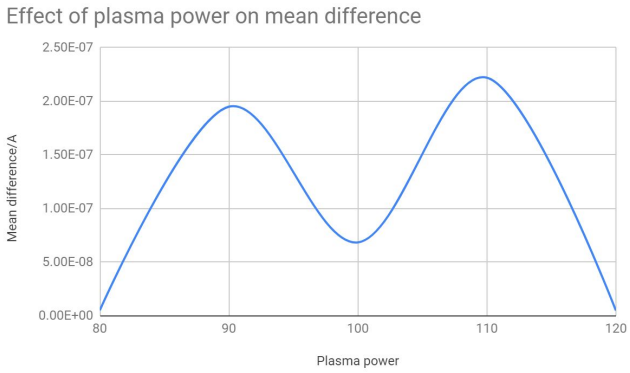

Fig 7. Mean difference against plasma power

4.3 Detection frequency

The setup used to determine the diode's peak detection frequency was similar, where the only difference was that the pulse rate of the LED light was now controlled by an electrical relay whose signal was generated by an electronic pulse generator. The pulse rate of the LED was gradually increased for each experiment while monitoring the light-to-dark ratio, and the maximum detection frequency achievable while ensuring reliable detection was determined for each sample. The pulse width and pulse spacing was varied using the pulse generator.

A change in current detected under a bias voltage of 1.0V corresponds the frequency in which the light is turned on and off. In Fig 8, a pulse width of 100ms was applied and the pulse spacing was changed from 100ms to 10ms then back to 100ms, which was detected by the graphene-silicon photodiode and shown in the difference in number of peaks within a certain time frame.

Fig 8. (above) Frequency test

Results were unable to be determined for pulse widths of under 100ns due to limitations in the pulse generator used. It was found that the silicon-graphene diode was able to detect for pulse spacings of as low as 1μs.

5 Conclusion

The data obtained from the experiment showed that the intensity of optoelectronic response in graphene-silicon diodes is inversely related to its physical proximity to the plasma source during hydrogenation; directly related to the power of the plasma, up to a point, after which it will deteriorate; and inversely related

This study contains possible limitations, *inter alia* random experimental errors, flaws in experimental design, and lack of depth, as more data would be necessary to produce a satisfactory and conclusive result. Further work is recommended, especially to:

- develop a process for more consistent diode fabrication;
- develop a process for more thorough removal of impurities introduced into the graphene during its transfer process;
- increase the low current generation by the photodiode when light is shone on it; and
- improve the poor lifespan of the effects of hydrogen functionalisation, as hydrogen atoms are lost to the environment within a short period of time.

The photodetection capabilities of the graphene-silicon diode demonstrated in this study show high promise for its future development as a novel alternative to traditional photodetectors, with the potential to bring great advancements in high-volume electronic communication.

References

Agrawal, G. P. (2012). Fiber-optic communication systems (Vol. 222). John Wiley & Sons.

An, Y., Behnam, A., Pop, E., & Ural, A. (2013). Metal-semiconductor-metal photodetectors based on graphene/p-type silicon Schottky junctions. Applied physics letters, 102(1), 013110.

Chen, C. C., Aykol, M., Chang, C. C., Levi, A. F. J., & Cronin, S. B. (2011). Graphene-silicon Schottky diodes. Nano letters, 11(5), 1863-1867.

Dey, A., Chroneos, A., Braithwaite, N. S. J., Gandhiraman, R. P., & Krishnamurthy, S. (2016). Plasma engineering of graphene. Applied Physics Reviews, 3(2), 021301.

Li, X., Magnuson, C. W., Venugopal, A., Tromp, R. M., Hannon, J. B., Vogel, E. M., Ruoff, R. S et al. (2011). Large-area graphene single crystals grown by low-pressure chemical vapor deposition of methane on copper. Journal of the American Chemical Society, 133(9), 2816-2819.

Pospischil, A., Humer, M., Furchi, M. M., Bachmann, D., Guider, R., Fromherz, T., & Mueller, T. (2013). CMOS-compatible graphene photodetector covering all optical communication bands. Nature Photonics, 7(11), 892.

Wang, C., Zhou, Y., He, L., Ng, T. W., Hong, G., Wu, Q. H., ... & Zhang, W. (2013). In situ nitrogen-doped graphene grown from polydimethylsiloxane by plasma enhanced chemical vapor deposition. Nanoscale, 5(2), 600-605.

Wang, X., Cheng, Z., Xu, K., Tsang, H. K., & Xu, J. B. (2013). High-responsivity graphene/silicon-heterostructure waveguide photodetectors. Nature Photonics, 7(11), 888.

Yan, R., Zhang, Q., Li, W., Calizo, I., Shen, T., Richter, C. A., ... & Grace Xing, H. (2012). Determination of graphene work function and graphene-insulator-semiconductor band alignment by internal photoemission spectroscopy. Applied Physics Letters, 101(2), 022105.

Zhang, X., Xie, C., Jie, J., Zhang, X., Wu, Y., & Zhang, W. (2013). High-efficiency graphene/Si nanoarray Schottky junction solar cells via surface modification and graphene doping. Journal of Materials Chemistry A, 1(22), 6593-6601.

Appendix

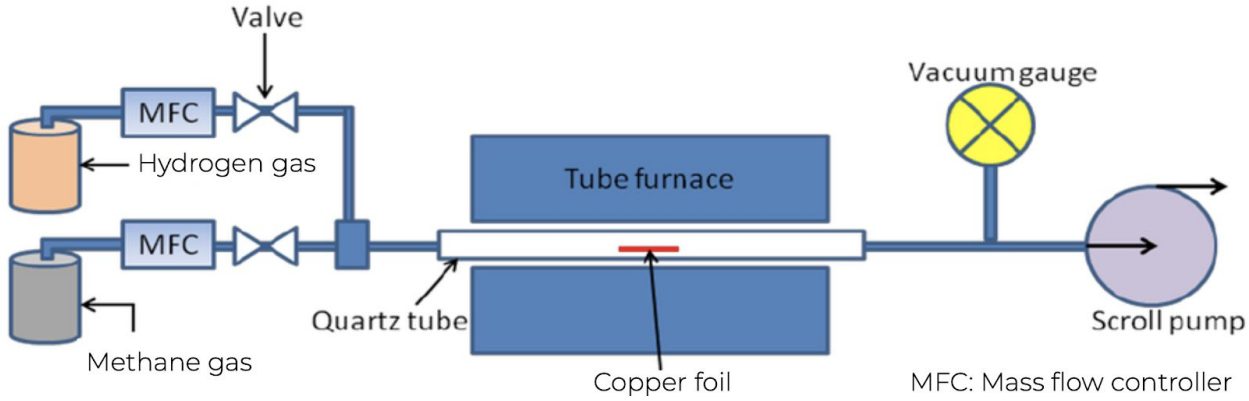

Fig 1. Diagram of CVD setup

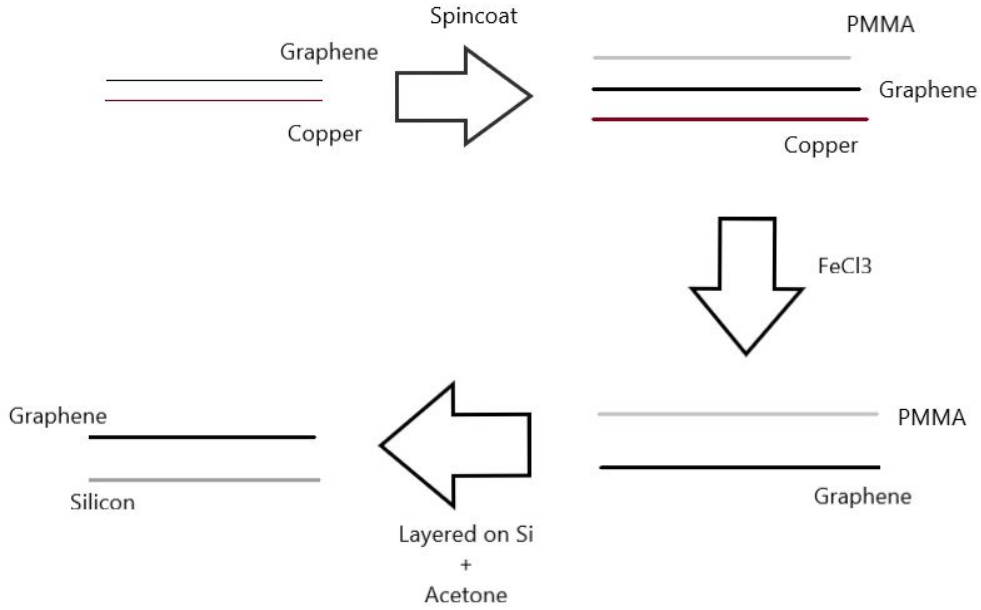

Fig 2. (above) Diagram of Transfer process

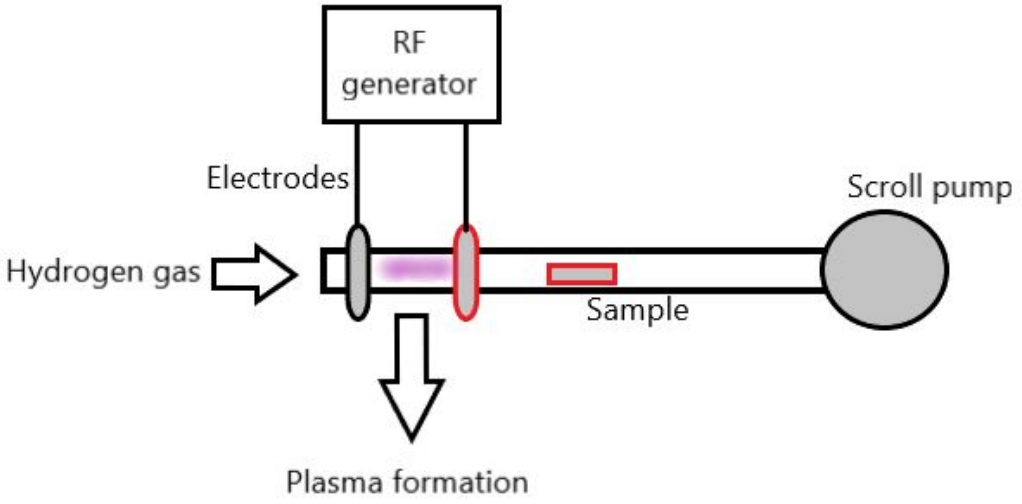

Fig 3. Diagram illustrating hydrogenation setup

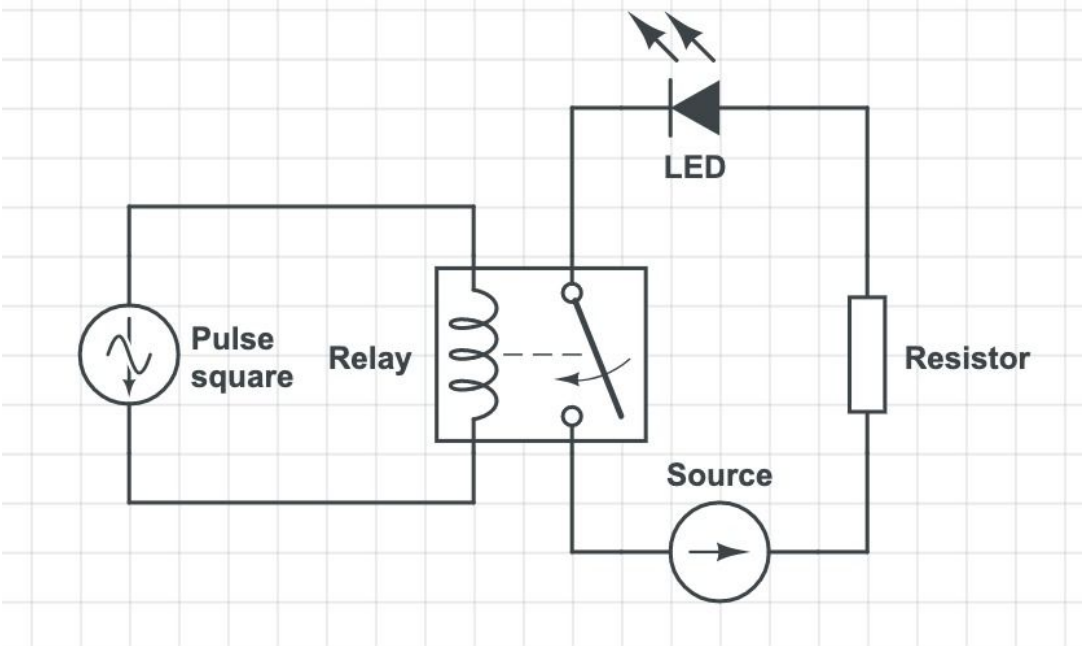

Fig 9. Diagram illustrating hydrogenation setup

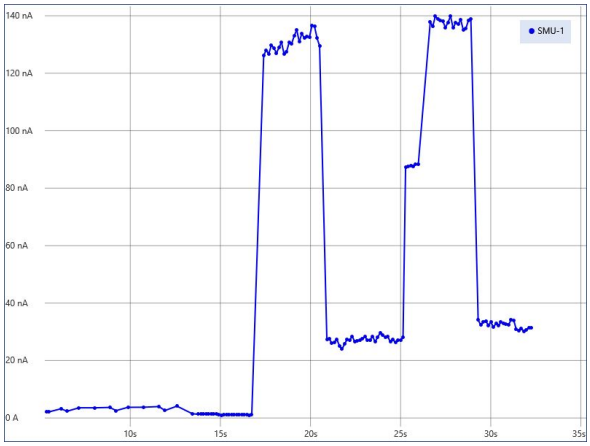
SMU-1
140 nA
120 nA
100 nA
80 nA
60 nA
40 nA
20 nA
0 A
10s
15s
20s
25s
30s
35s

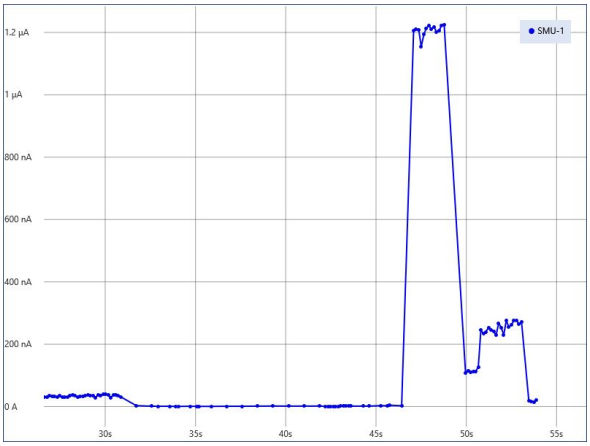
SMU-1
1.2 µA
1 µA
800 nA
600 nA
400 nA
200 nA
0 A
30s
35s
40s
45s
50s
55s

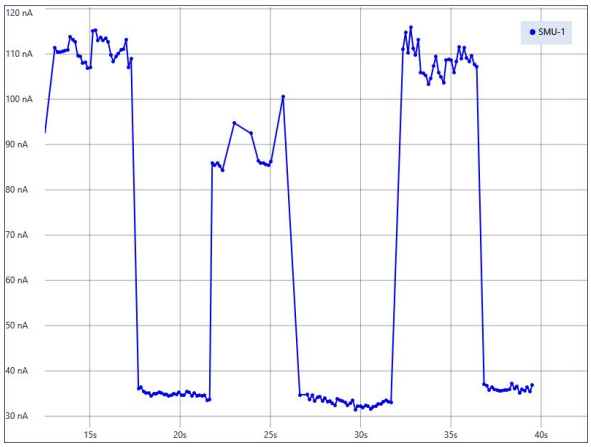
SMU-1
120 nA
110 nA
100 nA
90 nA
80 nA
70 nA
60 nA
50 nA
40 nA
30 nA
15s
20s
25s
30s
35s
40s

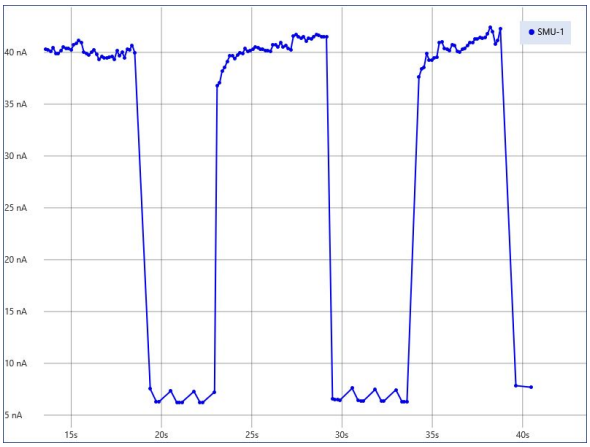
SMU-1
40 nA
35 nA
30 nA
25 nA
20 nA
15 nA
10 nA
5 nA
15s
20s
25s
30s
35s
40s

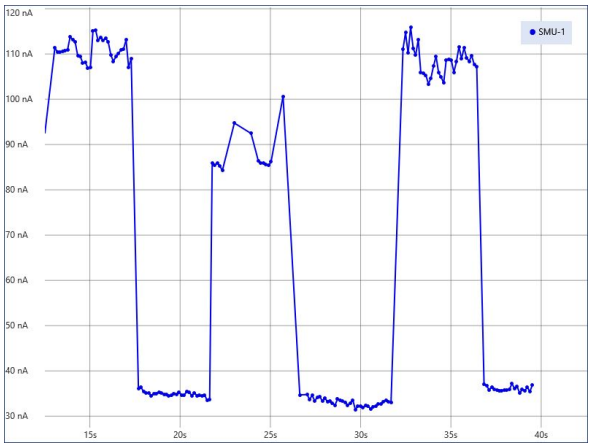
SMU-1
120 nA
110 nA
100 nA
90 nA
80 nA
70 nA
60 nA
50 nA
40 nA
30 nA
15s
20s
25s
30s
35s
40s

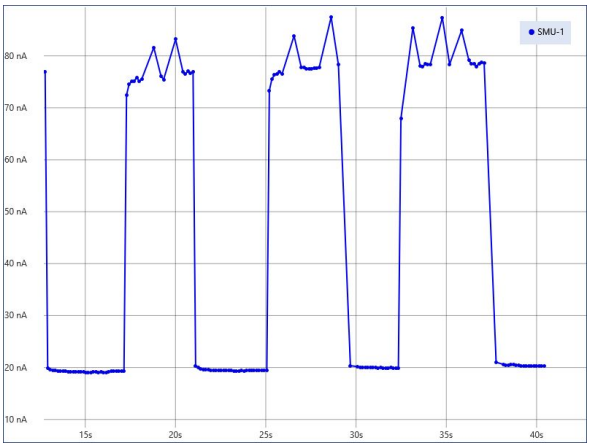
SMU-1
80 nA
70 nA
60 nA
50 nA
40 nA
30 nA
20 nA
10 nA
15s
20s
25s
30s
35s
40s

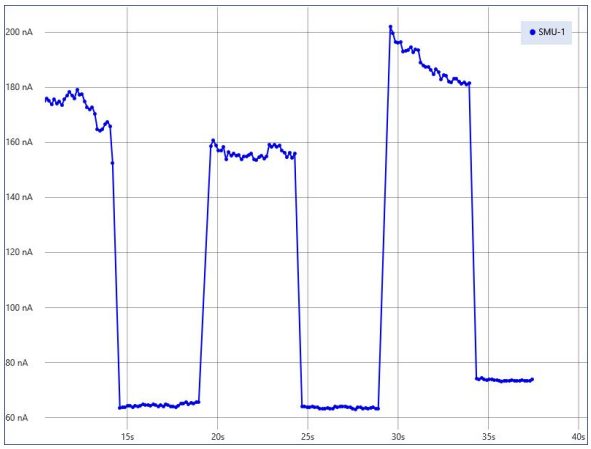
SMU-1
200 nA
180 nA
160 nA
140 nA
120 nA
100 nA
80 nA
60 nA
15s
20s
25s
30s
35s
40s

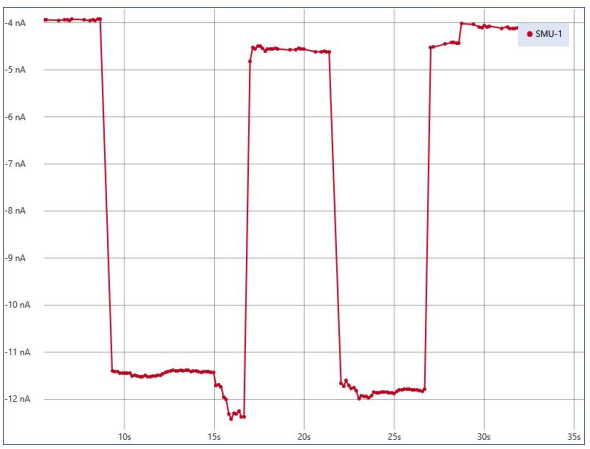
SMU-1
-4 nA
-5 nA
-6 nA
-7 nA
-8 nA
-9 nA
-10 nA
-11 nA
-12 nA
10s
15s
20s
25s
30s
35s

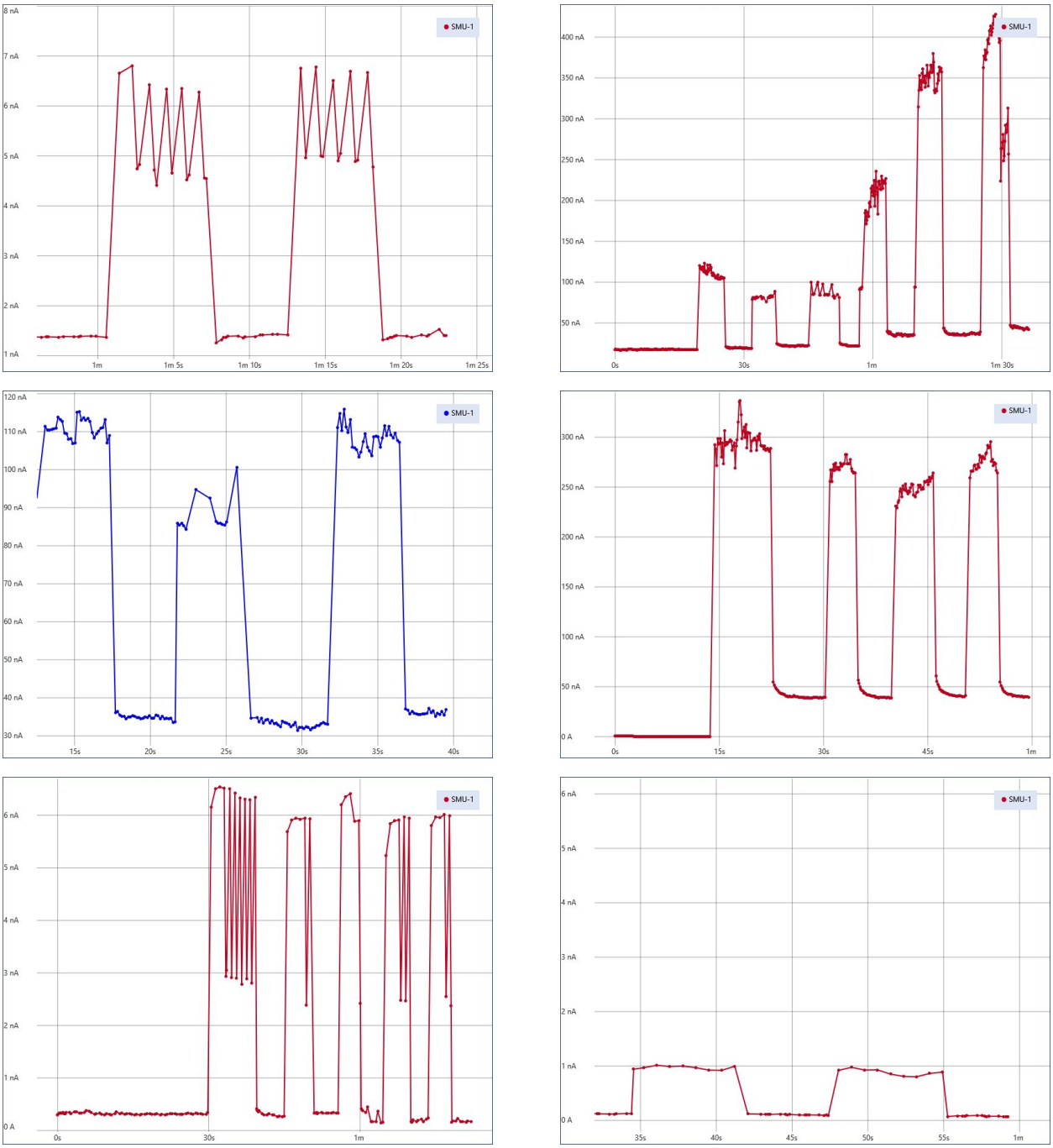

Fig 10 - 22. Graph of current for all experimental results, in the order they appear in Table 1.

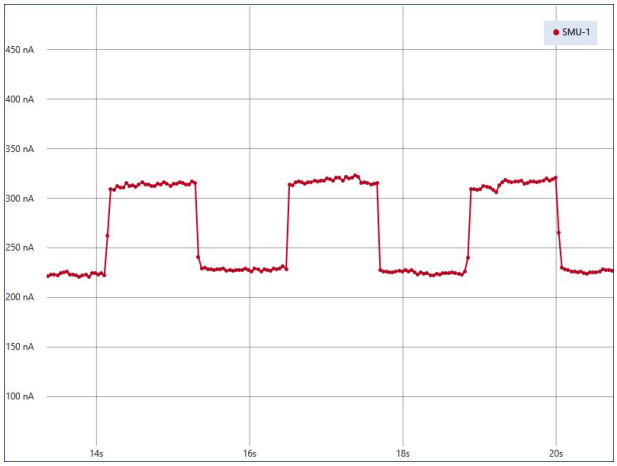

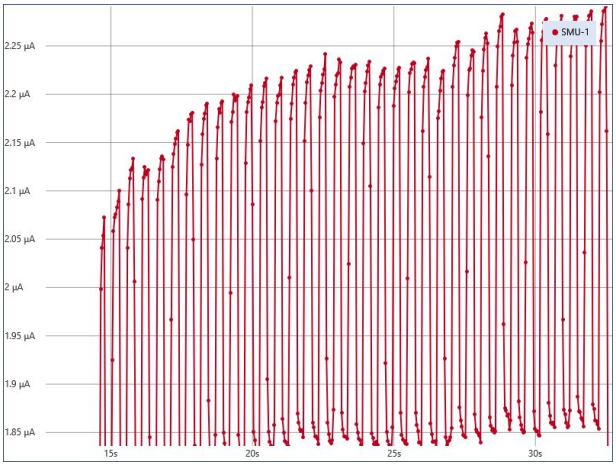

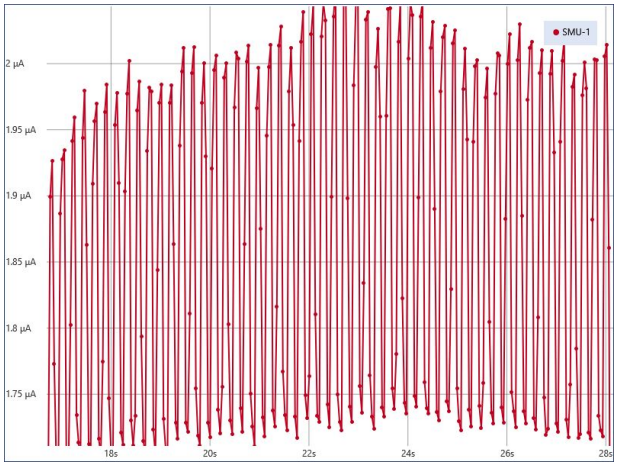

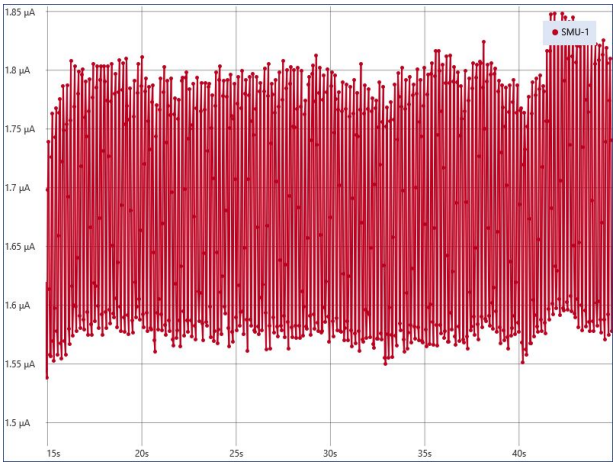

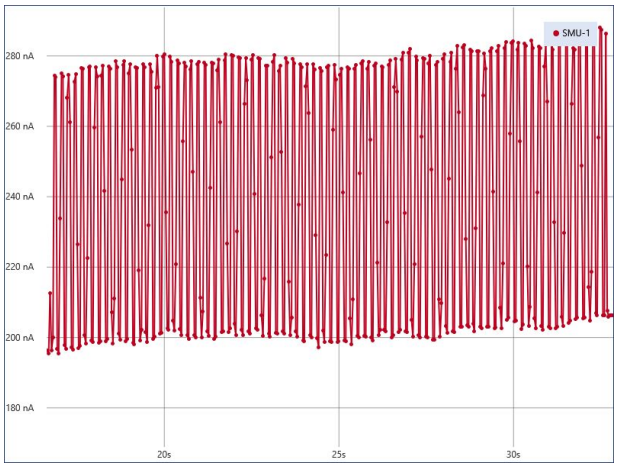

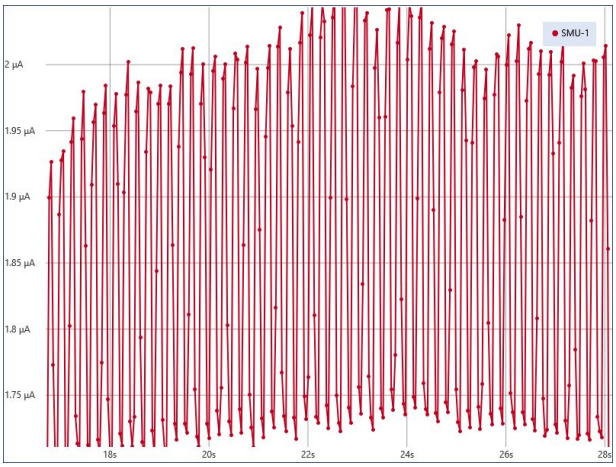

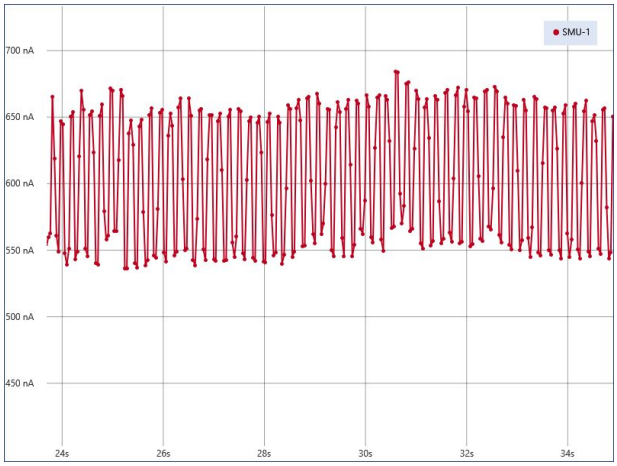

Fig 23 - 29. Current generated while varying pulse width and pulse space, respectively in order: 100ms, 100ms; 100ms, 10ms; 100ms, 1ms; 100ms, 100µs; 100ms, 10µs; 100ms, 1µs; 100ms, 100ns